



NRC Publications Archive Archives des publications du CNRC

Nonequilibrium stretching dynamics of dilute and entangled linear polymers in extensional flow

Kabanemi, Kalonji K.; Hétu, Jean-Francois

This publication could be one of several versions: author's original, accepted manuscript or the publisher's version. / La version de cette publication peut être l'une des suivantes : la version prépublication de l'auteur, la version acceptée du manuscrit ou la version de l'éditeur.

For the publisher's version, please access the DOI link below. / Pour consulter la version de l'éditeur, utilisez le lien DOI ci-dessous.

Publisher's version / Version de l'éditeur:

<https://doi.org/10.1016/j.jnnfm.2009.03.006>

Journal of Non-Newtonian Fluid Mechanics, 160, 2-3, pp. 113-121, 2009-08

NRC Publications Record / Notice d'Archives des publications de CNRC:

<https://nrc-publications.canada.ca/eng/view/object/?id=ead0f413-736d-4f46-b00f-faa9d97cf078>

<https://publications-cnrc.canada.ca/fra/voir/objet/?id=ead0f413-736d-4f46-b00f-faa9d97cf078>

Access and use of this website and the material on it are subject to the Terms and Conditions set forth at

<https://nrc-publications.canada.ca/eng/copyright>

READ THESE TERMS AND CONDITIONS CAREFULLY BEFORE USING THIS WEBSITE.

L'accès à ce site Web et l'utilisation de son contenu sont assujettis aux conditions présentées dans le site

<https://publications-cnrc.canada.ca/fra/droits>

LISEZ CES CONDITIONS ATTENTIVEMENT AVANT D'UTILISER CE SITE WEB.

Questions? Contact the NRC Publications Archive team at

PublicationsArchive-ArchivesPublications@nrc-cnrc.gc.ca. If you wish to email the authors directly, please see the first page of the publication for their contact information.

Vous avez des questions? Nous pouvons vous aider. Pour communiquer directement avec un auteur, consultez la première page de la revue dans laquelle son article a été publié afin de trouver ses coordonnées. Si vous n'arrivez pas à les repérer, communiquez avec nous à PublicationsArchive-ArchivesPublications@nrc-cnrc.gc.ca.



National Research
Council Canada

Conseil national de
recherches Canada

Canada



Nonequilibrium stretching dynamics of dilute and entangled linear polymers in extensional flow

Kalonji K. Kabanemi*, Jean-François Hétu

Industrial Materials Institute (IMI), National Research Council of Canada (NRC), 75 de Mortagne, Boucherville, Québec, Canada J4B 6Y4

ARTICLE INFO

Article history:

Received 19 January 2009

Received in revised form 13 March 2009

Accepted 17 March 2009

Keywords:

Entangled polymers
Dilute polymers
Stress–conformation hysteresis
Non-linear rheology
Extensional flow
Chain stretching

ABSTRACT

We propose an extension of the FENE-CR model for dilute polymer solutions [M.D. Chilcott, J.M. Rallison, Creeping flow of dilute polymer solutions past cylinders and spheres, *J. Non-Newtonian Fluid Mech.* 29 (1988) 382–432] and the Rouse-CCR tube model for linear entangled polymers [A.E. Likhtman, R.S. Graham, Simple constitutive equation for linear polymer melts derived from molecular theory: Rolie–Poly equation, *J. Non-Newtonian Fluid Mech.* 114 (2003) 1–12], to describe the nonequilibrium stretching dynamics of polymer chains in strong extensional flows. The resulting models, designed to capture the progressive changes in the average internal structure (kinked state) of the polymer chain, include an ‘effective’ maximum contour length that depends on local flow dynamics. The rheological behavior of the modified models is compared with various results already published in the literature for entangled polystyrene solutions, and for the Kramers chain model (dilute polymer solutions). It is shown that the FENE-CR model with an ‘effective’ maximum contour length is able to describe correctly the hysteretic behavior in stress versus birefringence in start-up of uniaxial extensional flow and subsequent relaxation also observed and computed by Doyle et al. [P.S. Doyle, E.S.G. Shaqfeh, G.H. McKinley, S.H. Spiegelberg, Relaxation of dilute polymer solutions following extensional flow, *J. Non-Newtonian Fluid Mech.* 76 (1998) 79–110] and Li and Larson [L. Li, R.G. Larson, Excluded volume effects on the birefringence and stress of dilute polymer solutions in extensional flow, *Rheol. Acta* 39 (2000) 419–427] using Brownian dynamics simulations of bead–spring model. The Rolie–Poly model with an ‘effective’ maximum contour length exhibits a less pronounced hysteretic behavior in stress versus birefringence in start-up of uniaxial extensional flow and subsequent relaxation.

Crown Copyright © 2009 Published by Elsevier B.V. All rights reserved.

1. Introduction

Experimental observations indicate that dilute and entangled polymer solutions display very different rheological behavior in extensional flows. Recently, Rothstein and McKinley [1,2] discussed, in depth, the role of the extensional rheology on vortex growth dynamics and the enhanced pressure drop during flow of a polystyrene Boger fluid through axisymmetric contraction–expansion geometry. They observed that the enhancement in the pressure drop was not associated with the onset of flow instability. They conjectured that this extra pressure drop is the result of an additional dissipative contribution to the polymeric stress arising from stress–conformation hysteresis in strong non-homogeneous extensional flow near contraction plane. Such a stress–conformation hysteresis was observed and computed by Doyle et al. [3] and Li and Larson [4] in transient uniaxial extensional flow, using Brownian dynamics simulations of bead–spring model. McKinley and Sridhar [5] and Larson

[6] have suggested that, at high-velocity gradients, the molecular individualism of polymer chains on the microscale becomes important and is reflected in the very heterogeneous population of conformations produced during these flows, as a result of the rapid and nonequilibrium nature of the stretching process.

On the other hand, Rothstein and McKinley [7] studied the stress and birefringence growth of a concentrated entangled polystyrene solution (labeled PS12) in uniaxial extensional flows. Contrary to the dilute polystyrene solution, they observed a less pronounced stress–conformation hysteresis during imposed stretching and subsequent stress relaxation at a strain rate of about, $\dot{\epsilon}_0 = 5.3 \text{ s}^{-1}$. They argued that, in order to observe a pronounced or measurable stress–conformation hysteresis, one would need to generate kinked configurations within each segment, and this would require a very strong flow ($\dot{\epsilon}_0 > 29 \text{ s}^{-1}$). Such deformation rates are not presently attainable in their filament-stretching rheometers.

It is therefore useful to focus effort on the definition of suitable and numerically tractable rheological constitutive models that could reproduce, at least, qualitatively the nonlinear viscoelastic behavior of dilute and entangled polymer solutions in rapidly changing flows.

* Corresponding author.

E-mail address: kalonji.kabanemi@cnrc-nrc.gc.ca (K.K. Kabanemi).

Various models for dilute polymer solutions have indeed been proposed that account for additional dissipative stress in strong extensional flows. Larson [6] developed kinks dynamics equations that describe the unraveling of the polymer chain in a strong extensional flow and found that large viscous stresses were produced. Hinch [8] showed that during the uncoiling, the stress is found to be mainly dissipative rather than elastic, i.e., the stress is proportional to the instantaneous strain rate rather than being independent of it. The contribution of a polymer chain to the stress tensor in the kinks dynamics model is dissipative, corresponding to the viscous dissipation as each segment of inextensible string fails to deform with the flow. He proposed a new expression for the stress, which is proportional to the strain rate. Rallison [9] further showed on the basis of molecular simulations the existence of a significant dissipative polymeric stress in planar extensional flow of a dilute polymer solution and proposed a natural extension of the finitely extensible nonlinear elastic (FENE-CR) equation that incorporates an additional stress term that has been chosen to be explicitly dissipative and proportional to the magnitude of the conformation tensor. Liekens et al. [10] addressed the closure approximation problem for the FENE dumbbell model. Inspired by stochastic simulation results for the FENE theory, they proposed a new model referred to as FENE-L. The new model was found to provide the best agreement with the FENE results. In particular, it is capable of reproducing the hysteretic behavior of the FENE model, in stress versus birefringence curves during start-up of flow and subsequent relaxation. More recently, Ghosh et al. [11] developed a new model for dilute polymer solutions in flows with strong extensional components. The new model, based on introducing an adaptive length scale (ALS) as an internal variable, was developed to reproduce the fine-scale physics of the Kramers chain model. The resulting ALS and ALS-C models give very good predictions of stress growth in start-up of uniaxial extensional flow and stress–birefringence hysteresis in a uniaxial extensional flow followed by relaxation.

In this work, we extend the FENE-CR model for dilute polymer solutions developed by Chilcott and Rallison [12] and the Rouse-convective constraint release (CCR) tube model for linear entangled polymers (Rolie–Poly equation), developed by Likhtman and Graham [13], by introducing the concept of ‘effective’ maximum contour length of polymer chains within the molecular theory, with the objective of capturing progressive changes in the average internal structure (kinked structure) of polymer chains, in strong uniaxial extensional flows. An alternative to this approach would be to include a spectrum of relaxation times in the model to represent the internal degrees of freedom. The theory, however, for general flows would be too complicated to be numerically tractable in a complex flow calculation, involving three-dimensional geometries.

The paper is organized as follows: We first present the original Rolie–Poly model by incorporating finite extensibility. Next, we analyze the behavior of the model in extensional flow and perform quantitative comparison with experimental data by Ye et al. [14]. In Section 4, we introduce the concept of effective maximum contour length in the Rolie–Poly model to describe the nonequilibrium stretching dynamics. The behavior of the extended model is then analyzed and compared with experimental data in Section 5. Finally, we introduce in Section 6, an extension of the FENE-CR model that includes the effective maximum contour length and compare its behavior, in extensional flow, with that of the Kramers chain model by Ghosh et al. [15].

2. Rouse–CCR tube model for linear entangled polymers with finite extensibility

In a recent paper dealing with the response of entangled polymer chains under rapid deformation, Graham et al. [16] proposed a molecular theory that does not need decoupling approxima-

tion, which leads to averages for orientation tensor and chain stretching. The resulting model includes the processes of reptation, CCR, reptation-driven constraint release, chain stretch and contour length fluctuations (CLF). Likhtman and Graham [13] derived from the full theory a simplified constitutive equation, which they called the Rolie–Poly constitutive equation, standing for Rouse linear entangled polymers. In that theory, the conformation of the polymer chain, σ , in a flow field, \mathbf{u} , evolves in time by an equation of the form

$$\dot{\sigma} = \mathbf{L} \cdot \sigma + \sigma \cdot \mathbf{L}^T + \mathbf{f}(\sigma), \quad (1)$$

where the tensor function, \mathbf{f} , is given by

$$\mathbf{f}(\sigma) = -\frac{1}{\tau_d}(\sigma - \mathbf{I}) - \frac{2}{\tau_R} \left(1 - \sqrt{\frac{3}{\text{tr} \sigma}} \right) \left(\sigma + \beta \left(\frac{\text{tr} \sigma}{3} \right)^\delta (\sigma - \mathbf{I}) \right). \quad (2)$$

Here $\mathbf{L} = \nabla \mathbf{u}^T$ is the transpose of velocity gradient tensor, τ_d is the fixed-tube disengagement time or reptation time, τ_R is the longest Rouse time or stretch time, β is the CCR coefficient analogous to the coefficient introduced by Marrucci [17] in his original CCR paper, δ is a negative power which can be obtained by fitting to the full theory, and $\sigma = \mathbf{I}$ is the equilibrium value of the conformation tensor in the absence of flow.

We want to emphasize here that neither theory [13,16] has finite extensibility included, which would limit the degree of strain hardening in the stretching regime. Indeed, non-Gaussian behavior cannot be ignored in fast flows, when chains stretch significantly. To account for finite extensibility of polymer chains into the original Rolie–Poly equation, we require that, in the absence of other relaxation mechanisms such as reptation and CCR, the trace of Eq. (1) leads to the relaxation for the stretch similarly as for the MLD model [18]. We then derive a non-Gaussian version of the Rolie–Poly constitutive equation, which accounts for finite extensibility of polymer chains, by writing the tensor function, \mathbf{f} , in the following form

$$\mathbf{f}(\sigma) = -\frac{1}{\tau_d}(\sigma - \mathbf{I}) - \frac{2}{\tau_R} k_s(\lambda) \left(1 - \sqrt{\frac{3}{\text{tr} \sigma}} \right) \times \left(\sigma + \beta \left(\frac{\text{tr} \sigma}{3} \right)^\delta (\sigma - \mathbf{I}) \right), \quad (3)$$

where $k_s(\lambda)$ is the nonlinear spring coefficient accounting for the finite extensibility of polymer chains, equals unity for linear springs and becomes much greater than unity as the spring becomes nearly fully stretched, and $\lambda = l/l_0 = \sqrt{\text{tr} \sigma}/3$ is the chain stretch ratio. The length, l , is the current tube length occupied by an entanglement segment and l_0 is the length of the same tube segment at equilibrium. $\lambda = 1$ is the equilibrium value in the absence of flow.

In the limit of large stretch and in the absence of any other relaxation mechanism, retraction, i.e., the trace of Eq. (1) with the expression for the tensor function, \mathbf{f} , given by Eq. (3), leads to the desired following relaxation for the stretch

$$\frac{d\lambda}{dt} = -\frac{1}{\tau_R} k_s(\lambda)(\lambda - 1). \quad (4)$$

This form was used in the MLD model with finite extensibility [19,20]. Note that in the limit of linear spring (Gaussian chain), $k_s(\lambda)$ remains unity, Eqs. (1) and (3) reduce to the original Rolie–Poly constitutive equation. The nonlinear spring coefficient, $k_s(\lambda)$, is approximated by the normalized Padé inverse Langevin function [20], i.e.,

$$k_s(\lambda) = \frac{(3 - \lambda^2/\lambda_{\max}^2)(1 - 1/\lambda_{\max}^2)}{(1 - \lambda^2/\lambda_{\max}^2)(3 - 1/\lambda_{\max}^2)}, \quad (5)$$

where λ_{\max} is the fixed maximum stretch ratio.

It is important to realize that in strong flows, when λ approaches λ_{\max} , the nonlinear spring coefficient, $k_s(\lambda)$, becomes very large and the 'effective' stretch relaxation time, $\tau_{\text{eff}} = \tau_R/k_s(\lambda)$, becomes shorter than the Rouse relaxation time, τ_R , and the evolution equation for the conformation tensor σ , Eq. (1), with the expression for the tensor function, f , given by Eq. (3), becomes difficult to solve numerically.

The constitutive equation, Eq. (1), with the expression for the tensor function, f , given by Eq. (3) is completed by specifying the relationship between the polymeric stress contribution τ_p and the conformation tensor σ .

For this purpose, let us recall that, the physical picture of the tube model is that the motion of any chosen polymer chain is strongly restricted by the presence of surrounding polymer chains, which creates a sort of a tube around the chosen chain. The contour length of the tube is given by the primitive chain length, consisting of Z primitive path steps (subchains or chain segments) which connect two consecutive entanglement points. At equilibrium, the average primitive path step or tube segment length, l_0 , is expected to be of the same order as the equilibrium tube diameter a_0 , and the equilibrium contour length of the whole tube is written as $L_0 = Z_0 l_0 = Z_0 a_0$, where Z_0 is the number of subchains (entanglements) per polymer chain at equilibrium. According to Gaussian chain statistics, $a_0 l_0 = N_{e0} b^2$ or $a_0^2 = N_{e0} b^2$, where b is the length of a 'monomer' or a Kuhn segment, N_{e0} is the number of monomers between entanglements at equilibrium and $N = Z_0 N_{e0}$ is the number of monomers per polymer chain. The stretch of the tube segment, $\lambda = l/l_0$, is assumed to be uniform along the chain contour length, where l is the nonequilibrium tube segment length. Assuming that the number of monomers in each subchain does not change during flow, the entropic force in each subchain is given by

$$F_{\text{FENE}}(\mathbf{R}) = \frac{3k_B T}{N_{e0} b^2} k_s \mathbf{R} = \frac{3k_B T}{a_0^2} k_s \mathbf{R}, \quad (6)$$

where \mathbf{R} is the end-to-end vector of the subchain, T is the absolute temperature and k_B is the Boltzmann constant. Assuming that the tube diameter stays constant and equal to its equilibrium value a_0 , the polymeric stress contribution due to traction along the tube axis, τ_p , is written as

$$\tau_p = cZ_0 \langle F_{\text{FENE}} \mathbf{R} \rangle = cZ_0 3k_B T k_s \frac{\langle \mathbf{R}\mathbf{R} \rangle}{a_0^2} = cN 3k_B T \frac{b^2}{a_0^2} k_s \frac{\langle \mathbf{R}\mathbf{R} \rangle}{a_0^2}. \quad (7)$$

Here the factor cZ_0 accounts for the number of subchains (entanglements) at equilibrium per unit volume, c is the number of polymer chains per volume and the factor cN accounts for the number of monomers per unit volume. In terms of the conformation tensor, σ , Eq. (7) can be written as

$$\tau_p = G k_s(\lambda)(\sigma - \mathbf{I}) = \frac{\eta_0}{\tau_d} k_s(\lambda)(\sigma - \mathbf{I}), \quad (8)$$

where $G = cZ_0 3k_B T = cN 3k_B T (b^2/a_0^2)$ is the plateau modulus and η_0 is the zero-shear-rate polymer viscosity. This equation ensures that at equilibrium, the polymer stress is zero. Finally, we define the refractive index tensor (birefringence), \mathbf{n} , as

$$\frac{\mathbf{n}}{C} = (\sigma - \mathbf{I}), \quad (9)$$

where C is the stress optical coefficient, which depends only on the local structure of the polymer chain.

3. Uniaxial extensional flow: linear entangled polymers

We here perform a quantitative comparison with the original Rolie-Poly model that does not include finite extensibility, in shear and uniaxial extensional flows, and calculate steady and transient extensional stress and extensional viscosity. We further include in

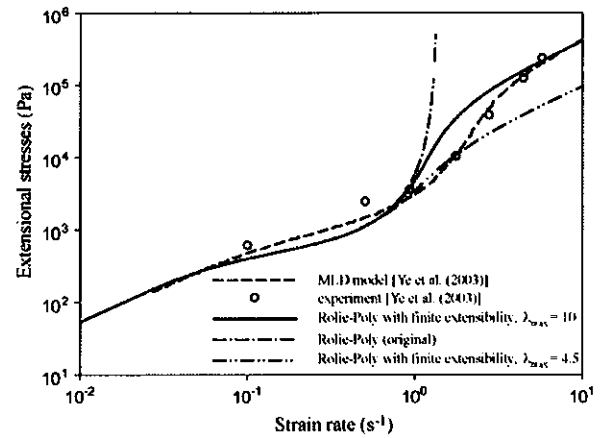


Fig. 1. Steady-state extensional stress prediction compared to that of the original Rolie-Poly model, the MLD model [14] and the experimental data for a nearly monodisperse linear polystyrene sample (L289) [14].

these comparisons, results of the MLD model and the experimental data by Ye et al. [14]. The polymer used is a nearly monodisperse linear polystyrene sample (L289) [14]. The following fluid parameters are used in the model: $\eta_0 = 1643.12$ Pa s, $\tau_d = 9.4$ s, $\tau_R = 0.76$ s, $\beta = 0.1$ and $\delta = -0.5$. The fixed maximum stretch ratio was adjusted arbitrarily to $\lambda_{\max} = 10$. The steady-state curves of the extensional stress are shown in Fig. 1. We further add in this figure predictions using a different value of the extensibility parameter of $\lambda_{\max} = 4.5$. At low strain rate for which $\dot{\epsilon} \tau_R \leq 1$, predictions are in good agreement with experimental data. In the stretching regime for which $\dot{\epsilon} \tau_R > 1$, however, predictions become sensitive to the value of the maximum stretch ratio and, the original Rolie-Poly fails, since it omits chain finite extensibility effects. The extensional stress is predicted to be linear in the rate of deformation at high $\dot{\epsilon} \tau_R$, for both the MLD model and the modified Rolie-Poly model. We would like to point out that, even with the modified Rolie-Poly model, quantitative agreement with experimental data is hardly achieved due to the simplification of single segment model, in which all chain segments are assumed to behave in the same way [21]. In Fig. 2, we compare the steady-state extensional viscosity for both models (Rolie-Poly model with and without finite extensibility). As noted by Ye et al. [14], the initial drop from the Newtonian value is due to tube orientation in the elongation direction. The extensional vis-

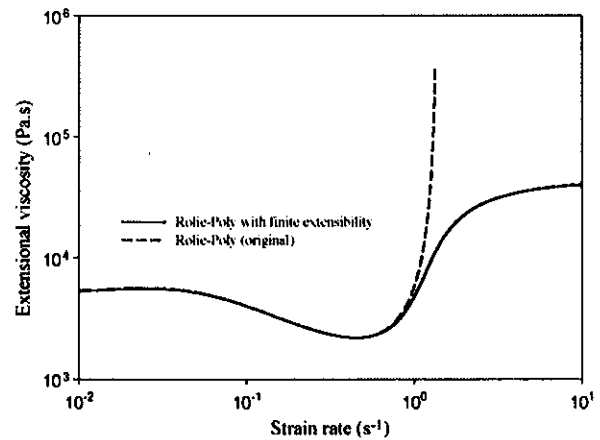


Fig. 2. Steady-state extensional viscosity prediction for the original Rolie-Poly model and the current Rolie-Poly model with finite extensibility, $\lambda_{\max} = 10$.

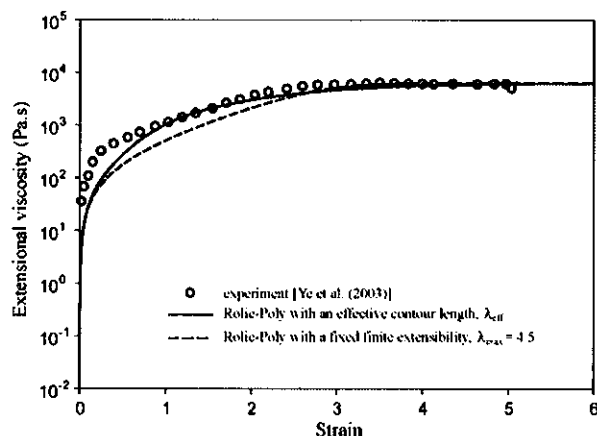


Fig. 3. Prediction of the transient extensional viscosity for the Rolie–Poly model with a fixed finite extensibility, λ_{\max} , and with an effective maximum contour length, λ_{eff} , compared to the experimental data for a nearly monodisperse linear polystyrene sample (L289) [14] at strain rate of $\dot{\epsilon} = 2 \text{ s}^{-1}$.

cosity is identical for both models at low strain rates. As strain rates increase ($\dot{\epsilon}\tau_R > 1$), chain stretch makes the viscosity increase. Contrary to the original Rolie–Poly model, the extensional viscosity reaches a final constant value due to the finite extensibility of polymer chain included in the current model.

In Fig. 3, we compare the prediction of the transient extensional viscosity, in start-up of uniaxial extensional flow to the experimental data for the same polystyrene by Ye et al. While the steady-state prediction is in agreement with the experimental data, the predicted stress growth at small strain, using the Rolie–Poly with λ_{\max} , is slower than the one measured experimentally. The effects of using an effective maximum contour length on the transient rheological behavior will be analyzed in the following section.

4. Nonequilibrium stretching dynamics for entangled polymers: ‘effective’ maximum contour length

In rapidly changing flows, the dynamics of the average quantity, σ , as described by Eq. (1), with the expression for the tensor function, f , given by Eq. (3), using the inverse Langevin force law, does not lead to accurate descriptions of changes in polymer chain configuration on significantly shorter length scales. Indeed, the inverse Langevin force law, obtained from equilibrium statistical mechanics, should be used with caution in nonequilibrium situations, in which the unfolding process of polymer chains takes place under nonequilibrium conditions.

Ianniruberto and Marrucci [21], in deriving their model for entangled polymers with chain stretch, pointed out that, when flow is fast enough to remove obstacles at rate faster than $1/\tau_R$, orientation and stretching relax together in a Rouse-like fashion. In other words, when at very high velocity gradients the intrinsic friction becomes dominant, each segment regains its own individuality. The test chain will change its conformation at a rate which only depends on the basic friction made by the chain with its surroundings. However, much less is known about the stress–conformation hysteresis in strong flows of entangled polymer solutions than their dilute solutions counterpart. The stress and birefringence growth of a concentrated entangled polystyrene solution (labeled PS12) in uniaxial extensional flows has been recently documented by Rothstein and McKinley [7]. Contrary to the dilute polystyrene solution, they observed a less pronounced stress–conformation hysteresis during imposed stretching and subsequent stress relaxation at a strain rate of about, $\dot{\epsilon}_0 = 5.3 \text{ s}^{-1}$. They pointed out that,

although the flow generated in the filament-stretching device was strong on the scale of the overall chain, it was weak on the level of the individual segment because $\tau_e \dot{\epsilon}_0 < 0.5$, where τ_e is the Rouse time for relaxation between entanglement points. It has been argued, however, that in order to observe a pronounced or measurable stress–conformation hysteresis, one would need to generate kinked configurations within each segment, and this would require a very strong flow ($\dot{\epsilon}_0 > 29 \text{ s}^{-1}$). Therefore, in the following, we mainly consider extensional flows in which the strain rates are large enough to result in strong nonequilibrium conformation of the polymer chain between entanglement points.

At strain rates, $\dot{\epsilon}$, that are low compared to the reciprocal Rouse time, τ_R , of the polymer chain, the chain conformation, at steady state, is nearly unperturbed from its equilibrium conformation. Distortion of the chain conformation occurs in strong extensional flows for which $\dot{\epsilon}\tau_R > 1$. In such a situation, the polymer chain can assume different nonequilibrium conformations to the final state that would not have occurred if the strain rate of the flow, $\dot{\epsilon}$, had been smaller than the reciprocal Rouse time τ_R . Under these conditions, the polymer chain undergoes conformational changes. This is very different from the corresponding equilibrium stretching situation.

To investigate such a complicated system, a simplified approach is used. In this aim, we introduce the concept of ‘effective’ maximum contour length to mimic the internal structure of a chain segment (subchain), i.e., kinked conformations and elongated coil within a single chain segment.

Before proceeding, let us recall that, the maximum length to which a tube segment can be stretched is given by $l_{\max} = 0.82n_e b_0$ (or equivalently, $\lambda_{\max} = l_{\max}/l_0$), where n_e is the number of backbone bonds in an entanglement spacing, b_0 the backbone bond length and l_0 the equilibrium tube segment length. We would like to emphasize here that, the pre-factor 0.82 and not 1 enters because the backbone has a zigzag configuration in the most extended state that still preserves the tetrahedral backbone bond angle restrictions [14]. This pre-factor has a direct incidence on the value of l_{\max} . In other words, it could change the flexibility of the chain. Therefore, parameters in the force law, Eq. (5), are directly related to the physical polymer chain. Since the kinked state seems to impede the molecular stretching, it is reasonable to assume that the coexistence of kinked conformations and elongated coil within a single chain segment reduces its flexibility and results in a shorter maximum length, which we call here ‘apparent’ or ‘effective’ maximum length, l_{eff} , to which a tube segment can be stretched.

Let us consider the situation where the polymer chain is stretched at a strain rate exceeding its reciprocal Rouse time τ_R , and let us suppose that, the polymer chain does not have the opportunity to fully relax the imposed deformation at each stage of stretching via reptation, retraction or CCR. Under these conditions, we conclude that, each chain segment will not have sufficient time to fully sample its configuration space and put forward the idea that kinked conformations and elongated coil will coexist within a single chain segment and will reduce its flexibility along with its maximum extensibility. In other words, only a fraction of the maximum contour length, l_{\max} , of the chain segment, identified by, l_{eff} , will be at equilibrium at each stage of stretching, otherwise the chain segment would be able to fully sample its configuration space at each stage of deformation. As a consequence, the chain segment is forced to stretch with a shorter effective maximum contour length, l_{eff} (or equivalently, $\lambda_{\text{eff}} = l_{\text{eff}}/l_0$), compared to the original fixed maximum contour length, l_{\max} . On average, this description, based on the effective maximum contour length, represents a coarse-grained approximation of internal conformation states (kinked conformations and elongated coil) of a chain segment during rapid stretching. If we identify this chain segment with a non-Gaussian chain, having a maximum contour length ratio,

λ_{eff} , then the nonlinear spring coefficient, obtained from equilibrium statistical mechanics, approximated by the normalized Padé inverse Langevin function, Eq. (5), can be used equivalently. Then the spring coefficient becomes

$$k_s(\lambda) = \frac{(3 - \lambda^2/\lambda_{\text{eff}}^2)(1 - 1/\lambda_{\text{eff}}^2)}{(1 - \lambda^2/\lambda_{\text{eff}}^2)(3 - 1/\lambda_{\text{eff}}^2)}. \quad (10)$$

Then, the next step is to calculate the effective maximum contour length ratio, λ_{eff} , under a given condition. By taking the trace of Eq. (1) in the absence of any relaxation mechanisms, flow generates a rate of stretch given by

$$\frac{d\lambda}{dt} = \frac{1}{3\lambda} \mathbf{L} : \boldsymbol{\sigma}. \quad (11)$$

The scalar quantity $(1/3\lambda)\mathbf{L} : \boldsymbol{\sigma}$, corresponds to the maximum instantaneous rate of stretch and is bounded above by $\dot{\epsilon}_g\lambda$, at each step of deformation, where $\dot{\epsilon}_g$ is the strain rate of the flow defined as

$$\dot{\epsilon}_g = \max |\text{eigenvalue}(\mathbf{d})|. \quad (12)$$

In Eq. (12), \mathbf{d} is the rate-of-deformation tensor defined by

$$\mathbf{d} = \frac{1}{2}(\nabla \mathbf{u} + \nabla \mathbf{u}^T). \quad (13)$$

Let us now take the trace of the full Eq. (1), including all relaxation mechanisms, i.e., with the expression for the tensor function, \mathbf{f} , given by Eq. (3). It gives

$$\frac{d\lambda}{dt} = \frac{1}{3\lambda} \mathbf{L} : \boldsymbol{\sigma} - \frac{1}{6\lambda} \mathbf{f}(\text{tr } \boldsymbol{\sigma}). \quad (14)$$

To better appreciate the crucial aspect of Eq. (14), we rewrite it in the following form

$$\left[1 - \frac{1}{(1/3\lambda)\mathbf{L} : \boldsymbol{\sigma}} \frac{d\lambda}{dt} \right] = \frac{(1/6\lambda)\mathbf{f}(\text{tr } \boldsymbol{\sigma})}{(1/3\lambda)\mathbf{L} : \boldsymbol{\sigma}}. \quad (15)$$

At equilibrium, as well as at low strain rates, for which $\dot{\epsilon}\tau_R \leq 1$, the chain conformational equilibrium is always maintained, therefore $(d\lambda/dt)/((1/3\lambda)\mathbf{L} : \boldsymbol{\sigma}) \approx 0$ in the left-hand side of Eq. (15), and the ratio on the right-hand side of Eq. (15) is close to unity. In other words, each chain segment will have sufficient time to fully sample its configuration space. In these flow conditions, since kinked state does not exist within each chain segment, its flexibility is not affected and the effective maximum contour length ratio, λ_{eff} , remains close to the fixed maximum contour length ratio, λ_{max} , at each stage of deformation. Since the unfolding process takes place under equilibrium conditions, the quantity $1 - (d\lambda/dt)/((1/3\lambda)\mathbf{L} : \boldsymbol{\sigma})$ is always close to unity; otherwise, the chain segment would not be able to fully sample its configuration space at each stage of deformation. From the above considerations, this quantity can also be interpreted as the fraction of the maximum length, l_{max} , at equilibrium, at each stage of deformation. Conversely, when in the limit of very high strain rate ($\dot{\epsilon}\tau_R \gg 1$), $(d\lambda/dt)/((1/3\lambda)\mathbf{L} : \boldsymbol{\sigma}) \approx 1$, the ratio on the right-hand side of Eq. (15) becomes close to zero, reflecting that each chain segment is driven into kinked state. In these flow conditions, the quantity $1 - (d\lambda/dt)/((1/3\lambda)\mathbf{L} : \boldsymbol{\sigma})$, which represents the fraction of l_{max} at equilibrium, at each stage of deformation, is close to zero. In other words, due to the presence of kinked state, the chain segment is 'frozen', its flexibility is considerably reduced and its apparent or effective maximum length, l_{eff} , becomes very small compared to l_{max} . In such conditions, the spring coefficient becomes sufficiently large to realize the 'quasi-inextensibility' of the chain segment.

More specifically, in strong extensional flows, for which $\dot{\epsilon}\tau_R > 1$, polymer chains are significantly stretched and the instantaneous rate of stretch is bounded, at each stage of stretching, by, $0 \leq$

$$|d\lambda/dt| \leq \dot{\epsilon}_g\lambda \text{ or equivalently}$$

$$0 \leq \frac{|d\lambda/dt|}{\dot{\epsilon}_g\lambda} \leq 1. \quad (16)$$

The above inequality represents in a sense, the fraction of l_{max} not at equilibrium, at each stage of deformation.

According to the conceptual scheme outline above, the ratio on the right-hand side of Eq. (15) represents the fraction of the polymer chain at equilibrium, at each stage of stretching. This leads to the following equation for the effective maximum contour length ratio

$$\lambda_{\text{eff}} = \left[1 - \frac{1}{\dot{\epsilon}_g\lambda} \left| \frac{d\lambda}{dt} \right| \right] (\lambda_{\text{max}} - 1) + 1. \quad (17)$$

Eq. (17) describes the coarse-grained internal conformation of the polymer chain molecule in strong extensional flows, by allowing a variation of the maximum contour length ratio of the chain segment at each stage of deformation. This equation contains a stretch term, $\dot{\epsilon}_g\lambda$, which leads to affine stretching of the polymer chain due to hydrodynamic drag. A second term, $|d\lambda/dt|$, governs the instantaneous stretch ratio dynamic, which is controlled by the Rouse time, τ_R .

In order for the model to always represent a polymer chain or a subchain of the same fixed maximum contour length ratio, λ_{max} , we introduce the number of 'sub-segments' defined as follows

$$M_s = \frac{\lambda_{\text{max}}}{\lambda_{\text{eff}}}. \quad (18)$$

We further assume a simplified situation where all chain segments behave in the same way, i.e., the orientation and lengths of all segments are identical. Therefore, the stress contribution of one segment must be multiplied by the number of segments to give the contribution of the macromolecules to the stress. On the basis of the above analysis, Eqs. (8) and (9) then generalize, respectively, to

$$\tau_p = M_s G k_s(\lambda)(\boldsymbol{\sigma} - \mathbf{I}) = M_s \frac{\eta_p}{\tau_d} k_s(\lambda)(\boldsymbol{\sigma} - \mathbf{I}) \quad (19)$$

and

$$\frac{\eta}{\dot{\epsilon}} = M_s(\boldsymbol{\sigma} - \mathbf{I}). \quad (20)$$

5. Uniaxial extensional flow: linear entangled polymers

In order to understand the behavior of the Rolie–Poly model with an effective maximum contour length ratio, λ_{eff} , we investigate the start-up results of uniaxial extensional flow. The fluid parameters are those of the entangled polystyrene solution used in Section 3 (L289) [14]. The calculated effective maximum contour length ratio, λ_{eff} , in uniaxial extensional flow is shown in Fig. 4 for various Weissenberg numbers, $Wi = \dot{\epsilon}\tau_R$. For $\dot{\epsilon}\tau_R < 1$, the chain conformation is nearly unperturbed from its equilibrium conformation and λ_{eff} does not deviate much from the fixed maximum contour length ratio, λ_{max} . At the same stretching rates, however, we observe a small decrease in λ_{eff} at the inception of flow, before it rapidly reaches the steady-state value, λ_{max} . This suggests that the polymer chain is generally in nonequilibrium conformation at low strains, during the stretching experiments. Conversely, for $\dot{\epsilon}\tau_R > 1$, significant nonequilibrium effects can be observed, and the effective maximum contour length ratio, λ_{eff} , immediately starts to decrease from its equilibrium value, λ_{max} , with increasing strain. This directly suggests that the chain segment (subchain) is driven into a kinked internal configuration state at these early stages of the flow. The extensibility of the polymer chain between entanglement points becomes restricted. Under these conditions, only a small fraction of the chain segment is under equilibrium up to a given strain, ϵ . At large strains, however, as the unraveling process proceeds, the chain

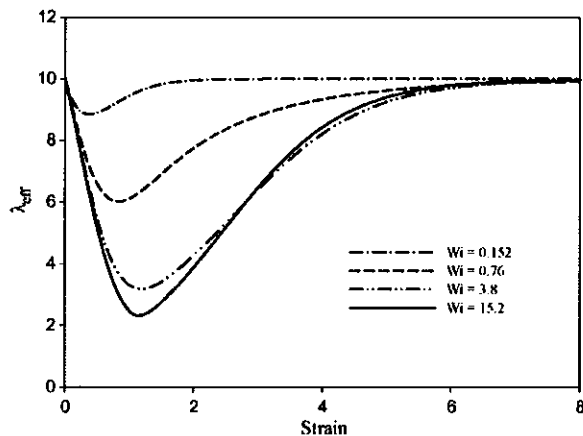


Fig. 4. Evolution of the effective maximum contour length ratio, λ_{eff} , with strain in start-up of uniaxial extensional flow, at various Weissenberg numbers, $Wi = \dot{\epsilon}\tau_R$, and with the fixed maximum contour length ratio, $\lambda_{\text{max}} = 10$.

segment becomes fully elongated and λ_{eff} tends to the fixed maximum contour length ratio, λ_{max} , reflecting that the overall polymer chain is under equilibrium. These phenomena result from different nonequilibrium conformations assumed by the chain segment during the unraveling process. Clearly, the current model is able to reproduce the time evolution of the average internal conformation of a chain segment, i.e., the effective maximum contour length ratio, λ_{eff} , during the entire flow process. The corresponding results for the chain stretch ratio, λ , as a function of the strain at various Weissenberg numbers, Wi , are shown in Fig. 5. As for the effective maximum contour length ratio, at low strain rates, the change from the equilibrium stretch ratio value, 1, is small. With increasing the strain rate, the chain stretch ratio approaches, λ_{max} , at large strain.

We now perform a quantitative comparison with the experimental data by Ye et al. [14], in uniaxial extensional flow, and calculate steady and transient extensional stress and extensional viscosity. The polymer used is a nearly monodisperse linear polystyrene sample (L842) [14]. The following fluid parameters are used in the model: $\eta_0 = 39 \times 10^3$ Pa s, $\tau_d = 192.7$ s, $\tau_R = 5$ s, $\beta = 0.1$ and $\delta = -0.5$. The fixed maximum stretch ratio was adjusted arbitrarily to $\lambda_{\text{max}} = 8$. The steady-state curves of the extensional stress are

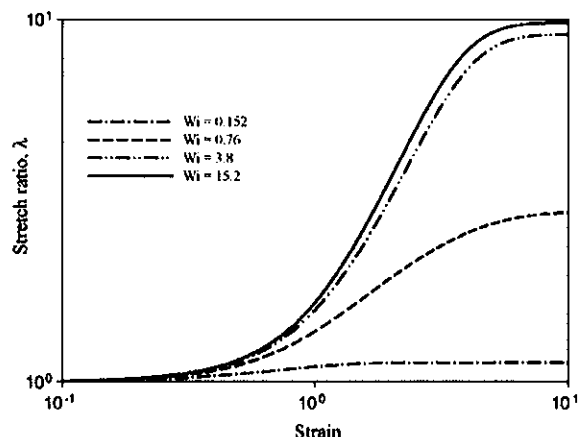


Fig. 5. Evolution of the chain stretch ratio, λ , with strain in start-up of uniaxial extensional flow, at various Weissenberg numbers, $Wi = \dot{\epsilon}\tau_R$, and with the fixed maximum contour length ratio, $\lambda_{\text{max}} = 10$.

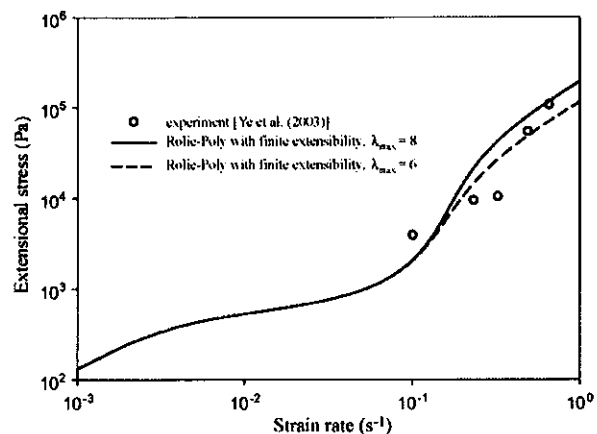


Fig. 6. Steady-state extensional stress prediction compared to the experimental data for a nearly monodisperse linear polystyrene sample (L842) [14].

shown in Fig. 6. We further add in this figure predictions using a different value of the extensibility parameter of $\lambda_{\text{max}} = 6$. As for the polystyrene L289, in the stretching regime for which $\dot{\epsilon}\tau_R > 1$, predictions become sensitive to the value of the maximum stretch ratio and, the extensional stress is predicted to be linear to the rate of deformation at high $\dot{\epsilon}\tau_R$.

Further insight into the results is provided in Figs. 3 and 7, where we compare the prediction of the transient extensional viscosity, in start-up of uniaxial extensional flow for the Rolie-Poly model with a fixed maximum contour length ratio, λ_{max} , and with an effective maximum contour length ratio, λ_{eff} , to the experimental data for L289 and L842 polystyrene samples by Ye et al. [14]. While the steady-state predictions are in agreement with the experimental data, the predicted stress growth at small strain using the Rolie-Poly model with a fixed maximum contour length ratio, λ_{max} , is slower than the one measured experimentally. The model with an effective contour length ratio, λ_{eff} , correctly predicts the stress growth at small strain. This is connected to special conformations of the subchains (kinked conformations between entanglement points) that build up during strong extensional flows.

We now consider the start-up of uniaxial extensional flow followed by relaxation for L842 polystyrene sample. The dependence

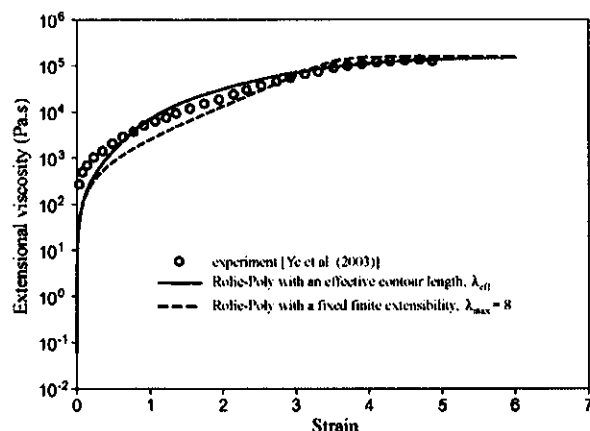


Fig. 7. Prediction of the transient extensional viscosity for the Rolie-Poly model with a fixed finite extensibility, λ_{max} , and with an effective maximum contour length, λ_{eff} , compared to the experimental data for a nearly monodisperse linear polystyrene sample (L842) [14] at strain rate of $\dot{\epsilon} = 0.5$ s $^{-1}$.

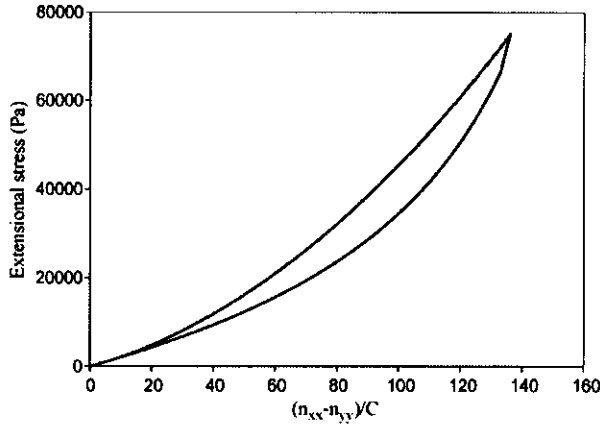


Fig. 8. Start-up of uniaxial extensional flow up to a final Hencky strain of $\varepsilon=6$, followed by relaxation: dependence of extensional stress on birefringence at $Wi = \dot{\varepsilon}\tau_R = 2.5$. The hysteresis curve is traveled clockwise.

of extensional stress on birefringence and stretch ratio, λ , at $Wi = \dot{\varepsilon}\tau_R = 2.5$ ($\dot{\varepsilon} = 0.5 \text{ s}^{-1}$) are shown in Figs. 8 and 9, respectively. The Rolie–Poly model with an effective maximum contour length ratio, λ_{eff} , exhibits a less pronounced stress–conformation hysteresis behavior at this strain rate. A qualitatively similar behavior has been reported in the experiments of Rothstein and McKinley [7], where the authors examined the stress–birefringence curves of their concentrated entangled polystyrene solution PS12. They reported a less pronounced hysteresis behavior in stress versus birefringence, compared with that of the dilute polystyrene solution PS025. They argued that, in order to observe a pronounced or measurable stress–conformation hysteresis, one would need to generate kinked configurations within each segment, and this would require a very strong flow. The model also shows hysteretic behavior in birefringence versus stretch ratio, as illustrated in Fig. 10. Although the current model predicts hysteretic behavior, all other predictions shown in the previous section, with a fixed maximum contour length ratio, λ_{max} , are not changed in steady state.

Summarizing the rheological predictions, we may conclude that the Rolie–Poly model with an effective maximum contour length ratio, λ_{eff} , is significantly better than the original Rolie–Poly model which does not include finite extensibility and therefore, can be

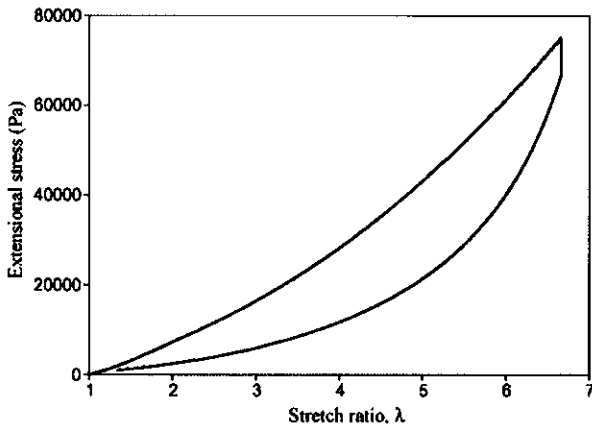


Fig. 9. Start-up of uniaxial extensional flow up to a final Hencky strain of $\varepsilon=6$, followed by relaxation: dependence of extensional stress on stretch ratio, λ , at $Wi = \dot{\varepsilon}\tau_R = 2.5$. The hysteresis curve is traveled clockwise.

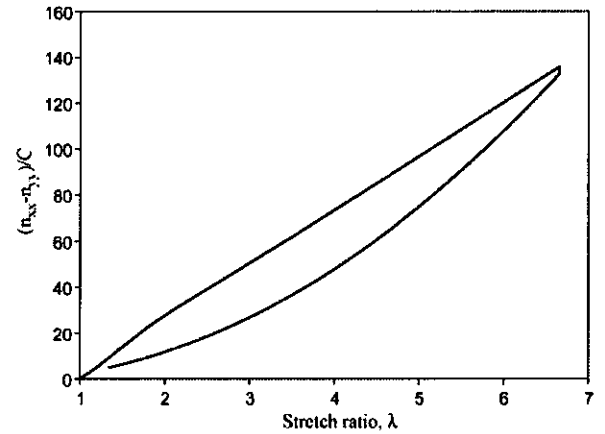


Fig. 10. Start-up of uniaxial extensional flow up to a final Hencky strain of $\varepsilon=6$, followed by relaxation: dependence of birefringence on stretch ratio, λ , at $Wi = \dot{\varepsilon}\tau_R = 2.5$. The hysteresis curve is traveled clockwise.

used to interpret future simulations of nonequilibrium complex flows.

6. Dilute polymer solutions: FENE-CR equation with an effective maximum contour length

For dilute polymer solutions, at strain rates, $\dot{\varepsilon}$, that are large compared to the longest relaxation time of the polymer chain, τ , the polymer chain can assume different nonequilibrium conformations to the final state that would not have occurred if the strain rate of the flow, $\dot{\varepsilon}$, had been smaller than the relaxation time, τ . In such a situation, molecular simulations show that, the polymer chain undergoes large conformational change and a pronounced stress–birefringence hysteresis is observed during stretching and relaxing processes [3,4]. As pointed out by Larson [6] in deriving kink dynamics equations that describe the unraveling of the molecule in extensional flow, flexible polymer chains in dilute solution, in transient extensional flows, experience a very strong drag force well before the chains are fully extended. He observed that soon after onset of a strong extensional flow, the polymer molecule is driven into a highly folded or kinked state.

To investigate such a problem, we write the constitutive equation for the FENE-CR fluid for dilute polymer solutions in the form introduced by Chilcott and Rallison [12] by incorporating the effective maximum length of a polymer chain, λ_{eff} , introduced in the previous section, in the following way:

$$\dot{\sigma} = \mathbf{L} \cdot \sigma + \sigma \cdot \mathbf{L}^T - \frac{k_s(\lambda)}{\tau}(\sigma - \mathbf{I}), \quad (21)$$

where τ is the relaxation time and $k_s(\lambda)$ is the nonlinear spring coefficient, which is also approximated by the normalized Padé inverse Langevin function defined by Eq. (10), and $\lambda = L/L_0 = \sqrt{\text{tr } \sigma}/3$ is the chain stretch ratio. The length, L , is the current length of the polymer chain and L_0 is its length at equilibrium and $\lambda = 1$ is the equilibrium value in the absence of flow. We would like to emphasize here that the dynamics of the conformation tensor, σ , is now governed by Eq. (21) and the effective maximum contour length ratio, λ_{eff} , has the same form as Eq. (17), i.e.,

$$\lambda_{\text{eff}} = \left[1 - \frac{1}{\dot{\varepsilon}_g \lambda} \left| \frac{d\lambda}{d\tau} \right| \right] (\lambda_{\text{max}} - 1) + 1. \quad (22)$$

The corresponding total stress, τ_T , in the solution is taken to be of the form

$$\tau_T = -p\mathbf{I} + 2\eta_s \mathbf{d} + \tau_p, \quad (23)$$

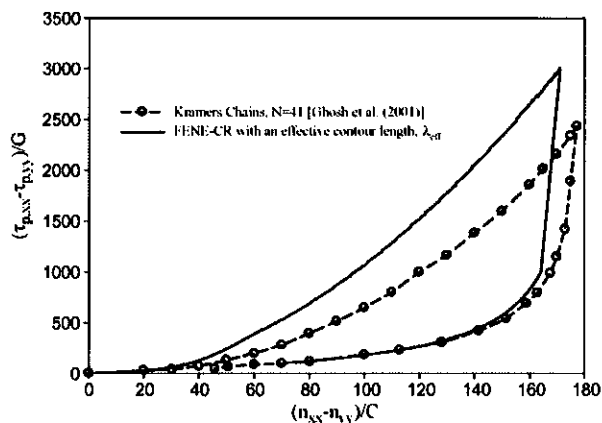


Fig. 11. Start-up of uniaxial extensional flow up to $\varepsilon = 5$ followed by relaxation for $N = 41$ Kramers chains [15] and FENE-CR with an effective maximum contour length, λ_{eff} . Dependence of extensional stress on birefringence at $Wi = \varepsilon\tau = 11.4$. The hysteresis curves are traveled clockwise.

where η_s is the solvent viscosity, \mathbf{d} the rate-of-deformation tensor and $\boldsymbol{\tau}_p$ the polymeric stress tensor, given by

$$\boldsymbol{\tau}_p = M_s G k_s(\lambda)(\boldsymbol{\sigma} - \mathbf{I}), \quad (24)$$

where $G = \eta_p/\tau$ is the plateau modulus and η_p is a viscosity coefficient. In order for the model to always represent a polymer chain of the same fixed maximum length ratio, λ_{max} , Eq. (24) has a factor, $M_s = \lambda_{\text{max}}/\lambda_{\text{eff}}$, which defines the number of 'sub-segments' and $M_s = 1$ is the equilibrium value in the absence of flow. To assess the validity of the extended FENE-CR model, we compare in Fig. 11, hysteresis curves of extensional stress versus birefringence, in start-up of uniaxial extensional flow up to $\varepsilon = 5$ followed by relaxation, for $N = 41$ Kramers chain model [15] and the FENE-CR model with an effective maximum contour length, λ_{eff} , at $Wi = \varepsilon\tau = 11.4$. The relaxation time, τ , is set to 3.24 s and the maximum stretch ratio was adjusted arbitrarily to $\lambda_{\text{max}} = 7.9$. The predicted stress-birefringence hysteresis using the current model shows excellent agreement with the Kramers chain model. In addition, we note from Fig. 11 that the two models traverse the hysteresis loop at a rate that is very similar, suggesting a strong nonequilibrium conformation of polymer chains. The growth of

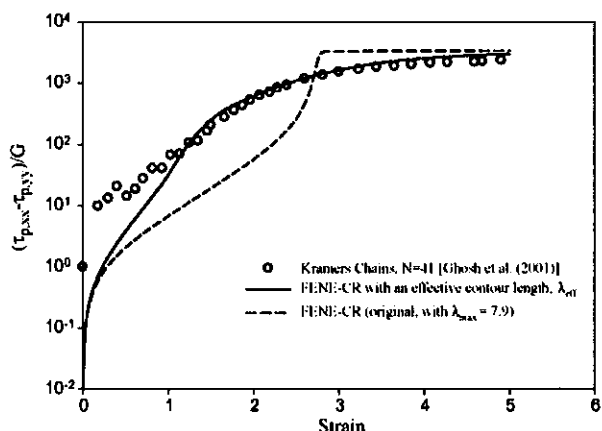


Fig. 12. Start-up of uniaxial extensional flow up to $\varepsilon = 5$ for $N = 41$ Kramers chains [15], FENE-CR with an effective maximum contour length, λ_{eff} and the original FENE-CR model with $\lambda_{\text{max}} = 7.9$. Dependence of extensional stress on strain at $Wi = \varepsilon\tau = 11.4$.

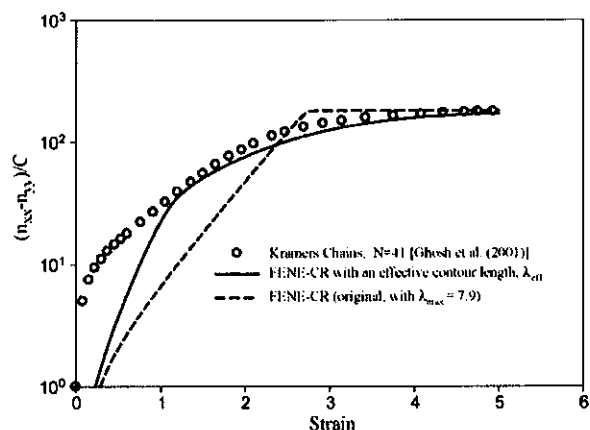


Fig. 13. Start-up of uniaxial extensional flow up to $\varepsilon = 5$ for $N = 41$ Kramers chains [15], FENE-CR with an effective maximum contour length, λ_{eff} , and the original FENE-CR model with $\lambda_{\text{max}} = 7.9$. Dependence of birefringence on strain at $Wi = \varepsilon\tau = 11.4$.

extensional stress and birefringence with strain in start-up of uniaxial extensional flow are compared to that of Kramers chain model in Figs. 12 and 13, respectively. While the extensional stress and birefringence predictions for the FENE-CR model are in good agreement with those of the Kramers chain model, these properties are predicted to rise less rapidly at low strain for the FENE-CR model with a fixed maximum contour length ratio, λ_{max} . The FENE-CR model with an effective contour length ratio, λ_{eff} , correctly predicts the stress growth at small strain.

7. Conclusions

We have presented an extension of the FENE-CR model for dilute polymer solutions and the Rouse-CCR tube model for linear entangled polymers (Rolie-Poly constitutive equation), to describe the nonequilibrium stretching dynamics of polymer chains in strong extensional flows. The resulting models, designed to capture the progressive changes in the average internal structure (kinked state) of the polymer chain, include an 'effective' maximum contour length that depends on local flow dynamics. The rheological behavior of the two models was favorably compared with various results already published in the literature for the entangled polystyrene solutions [14] and for the Kramers chain model [15]. It was shown that the FENE-CR model with an 'effective' maximum contour length is able to describe correctly the hysteretic behavior in stress versus birefringence in start-up of uniaxial extensional flow and subsequent relaxation also observed and computed by Doyle et al. [3] and Li and Larson [4] using Brownian dynamics simulations of bead-spring model. For linear entangled polymers, the Rolie-Poly model, with an 'effective' maximum contour length, exhibits a less pronounced hysteretic behavior in stress versus birefringence in start-up of uniaxial extensional flow and subsequent relaxation.

References

- [1] J.P. Rothstein, G.H. McKinley, Extensional flow of a polystyrene Boger fluid through a 4:1:4 axisymmetric contraction/expansion, *J. Non-Newtonian Fluid Mech.* 86 (1999) 61–88.
- [2] J.P. Rothstein, G.H. McKinley, The axisymmetric contraction-expansion: the role of extensional rheology on vortex growth dynamics and the enhanced pressure drop, *J. Non-Newtonian Fluid Mech.* 98 (2001) 33–63.
- [3] P.S. Doyle, E.S.G. Shaqfeh, G.H. McKinley, S.H. Spiegelberg, Relaxation of dilute polymer solutions following extensional flow, *J. Non-Newtonian Fluid Mech.* 76 (1998) 79–110.
- [4] L. Li, R.G. Larson, Excluded volume effects on the birefringence and stress of dilute polymer solutions in extensional flow, *Rheol. Acta* 39 (2000) 419–427.

- [5] G.H. McKinley, T. Sridhar, Filament-stretching rheometry of complex fluids, *Annu. Rev. Fluid Mech.* 34 (2002) 375–415.
- [6] R.G. Larson, The unravelling of a polymer chain in a strong extensional flow, *Rheol. Acta* 29 (1990) 371–384.
- [7] J.P. Rothstein, G.H. McKinley, A comparison of the stress and birefringence growth of dilute, semi-dilute and concentrated polymer solutions in uniaxial extensional flows, *J. Non-Newtonian Fluid Mech.* 108 (2002) 275–290.
- [8] E.J. Hinch, Uncoiling a polymer molecule in a strong extensional flow, *J. Non-Newtonian Fluid Mech.* 54 (1994) 209–230.
- [9] J.M. Rallison, Dissipative stresses in dilute polymer solutions, *J. Non-Newtonian Fluid Mech.* 68 (1997) 61–83.
- [10] G. Lielens, P. Halin, I. Jaumain, R. Keunings, V. Legat, New closure approximations for kinetic theory of finitely extensible dumbbells, *J. Non-Newtonian Fluid Mech.* 76 (1998) 249–279.
- [11] I. Ghosh, Y.L. Joo, G.H. McKinley, R.A. Brown, R.C. Armstrong, A new model for dilute polymer solutions in flows with strong extensional components, *J. Rheol.* 46 (2002) 1057–1089.
- [12] M.D. Chilcott, J.M. Rallison, Creeping flow of dilute polymer solutions past cylinders and spheres, *J. Non-Newtonian Fluid Mech.* 29 (1988) 382–432.
- [13] A.E. Likhtman, R.S. Graham, Simple constitutive equation for linear polymer melts derived from molecular theory: Rolie-Poly equation, *J. Non-Newtonian Fluid Mech.* 114 (2003) 1–12.
- [14] X. Ye, R.G. Larson, C. Pattamaprom, T. Sridhar, Extensional properties of monodisperse and bidisperse polystyrene solutions, *J. Rheol.* 47 (2003) 443–468.
- [15] I. Ghosh, G.H. McKinley, R.A. Brown, R.C. Armstrong, Deficiencies of FENE dumbbell models in describing the rapid stretching of dilute polymer solutions, *J. Rheol.* 45 (2001) 721–758.
- [16] R.S. Graham, A.E. Likhtman, T.C.B. McLeish, S.T. Milner, Microscopic theory of linear, entangled polymer chains under rapid deformation including chain stretch and convective constraint release, *J. Rheol.* 47 (2003) 1171–1200.
- [17] G. Marrucci, Dynamics of entanglements: a nonlinear model consistent with the Cox-Merz rule, *J. Non-Newtonian Fluid Mech.* 62 (1996) 279–289.
- [18] D.W. Mead, R.G. Larson, M. Doi, A molecular theory for fast flows of entangled polymers, *Macromolecules* 31 (1998) 7895–7914.
- [19] C. Pattamaprom, R.G. Larson, Constraint release effects in monodisperse and bidisperse polystyrenes in fast transient shearing flows, *Macromolecules* 34 (2001) 5229–5237.
- [20] C. Pattamaprom, J.J. Driscoll, R.G. Larson, Nonlinear viscoelastic predictions of uniaxial-extensional viscosities of entangled polymers, *Macromol. Symp.* 158 (2000) 1–13.
- [21] G. Ianniruberto, G. Marrucci, A multi-mode CCR model for entangled polymers with chain stretch, *J. Non-Newtonian Fluid Mech.* 102 (2002) 383–395.